

X6.9-CLASS FLARE-INDUCED VERTICAL KINK OSCILLATIONS IN A LARGE-SCALE PLASMA CURTAIN AS OBSERVED BY THE *SOLAR DYNAMICS* *OBSERVATORY*/ATMOSPHERIC IMAGING ASSEMBLY

A. K. SRIVASTAVA¹ AND M. GOOSSENS²

¹ Aryabhata Research Institute of Observational Sciences (ARIES), Manora Peak, Nainital 263 002, India

² Centre for Mathematical Plasma Astrophysics, Department of Mathematics, KU Leuven,
Celestijnenlaan 200B, B-3001 Leuven, Belgium

Received 2013 April 14; accepted 2013 August 26; published 2013 October 9

ABSTRACT

We present rare observational evidence of vertical kink oscillations in a laminar and diffused large-scale plasma curtain as observed by the Atmospheric Imaging Assembly on board the *Solar Dynamics Observatory*. The X6.9-class flare in active region 11263 on 2011 August 9 induces a global large-scale disturbance that propagates in a narrow lane above the plasma curtain and creates a low density region that appears as a dimming in the observational image data. This large-scale propagating disturbance acts as a non-periodic driver that interacts asymmetrically and obliquely with the top of the plasma curtain and triggers the observed oscillations. In the deeper layers of the curtain, we find evidence of vertical kink oscillations with two periods (795 s and 530 s). On the magnetic surface of the curtain where the density is inhomogeneous due to coronal dimming, non-decaying vertical oscillations are also observed (period \approx 763–896 s). We infer that the global large-scale disturbance triggers vertical kink oscillations in the deeper layers as well as on the surface of the large-scale plasma curtain. The properties of the excited waves strongly depend on the local plasma and magnetic field conditions.

Key words: magnetohydrodynamics (MHD) – Sun: corona – Sun: flares – Sun: oscillations

Online-only material: color figures, animation

1. INTRODUCTION

The major concern of this paper is to understand the conditions for the excitation of vertical kink oscillations in a diffused and large-scale laminar plasma curtain. Kink MHD waves are exceptional in the sense that they are the only waves that displace the axis of a magnetic tube and the tube as a whole. For that reason the standing transverse MHD waves observed in coronal loops are interpreted as standing MHD kink waves. Apart from the transverse kink waves, there are claims that torsional Alfvén waves have been detected in various magnetic structures at diverse spatial scales in the solar atmosphere (e.g., Erdélyi & Fedun 2007; Jess et al. 2009 and references therein). The observed Alfvén waves are potential candidates for heating the solar corona locally as well as for pursuing MHD seismology of the localized atmosphere (Harrison et al. 2002; Dwivedi & Srivastava 2006; Jess et al. 2009; Morton et al. 2011; De Moortel & Nakariakov 2012; Mathioudakis et al. 2013 and references therein).

Horizontal kink oscillations triggered by flares have been observed in imaging observations of solar loops since the era of TRACE followed by *Hinode*, *STEREO*, and the *Solar Dynamics Observatory* (SDO; e.g., Aschwanden et al. 1999; Nakariakov et al. 1999; Van Doorsselaere et al. 2008; Verwichte et al. 2009; Aschwanden & Schrijver 2011; Srivastava et al. 2013 and references therein). Spectroscopic observations of kink waves are also reported for flaring and non-flaring active region loops (O’Shea et al. 2007; Erdélyi & Taroyan 2008; Van Doorsselaere et al. 2008; Andries et al. 2009) using, respectively, the Coronal Diagnostics Spectrometer on *SOHO* and the EUV Imaging Spectrometer on *Hinode*. Observations of kink waves are used to obtain estimates of plasma properties and of local physical conditions of the solar corona (Nakariakov & Ofman 2001; Goossens et al. 2002a; Andries et al. 2005a, 2005b; Arregui

et al. 2007; Goossens 2008; Andries et al. 2009). These weakly compressible kink waves are also observed in the stellar corona of ξ -Boo (Pandey & Srivastava 2009; Anfinogentov et al. 2013).

Vertical kink waves have been detected in the solar atmosphere since mid-2000, but only a few cases are known so far (e.g., Wang & Solanki 2004; Li & Gan 2006; Aschwanden & Schrijver 2011; White et al. 2012 and references therein). White et al. (2012) recently reported flare-induced vertical kink oscillations in an eruptive loop in the vicinity of a vertical current sheet. The off-limb coronal loop observed by White et al. (2012) is very symmetric and elliptical, and the flare disturbances that triggered the vertical kink wave occurred just below the apex of the loop somewhere near the limb. Selwa et al. (2011) claim that the excitation of vertical kink oscillations depends on the symmetry of the loop with respect to its interaction with the localized periodic drivers. They argue that the absence of symmetry prevents vertical kink modes while horizontal kink oscillations can be excited. Selwa et al. (2011) used this argument to explain why vertical kink oscillation are so rarely observed in the solar corona. Aschwanden & Schrijver (2011) have found that vertical kink oscillations can be triggered by flare-generated fast MHD waves. The propagation and interaction of large-scale coronal waves as well as coronal mass ejections (CMEs) can also trigger kink oscillations in the solar loops (e.g., Liu et al. 2011, 2012; Wang et al. 2012). Several theoretical and numerical investigations have tried to understand the vertical and horizontal polarized kink oscillations of coronal loops in the MHD regime (e.g., Gruszecki et al. 2006; McLaughlin & Ofman 2008; Selwa et al. 2007; Selwa & Ofman 2010 and references therein). The onset of the appropriate triggering mechanism and physical conditions to excite the vertical kink oscillations is rare in the solar corona (Selwa et al. 2011; White et al. 2012). Therefore, there are only a few observational reports in the context of the evolution of vertical kink oscillations in the solar atmosphere.

However, occasional limitations in the observational base line may make the identification of these vertical kink oscillations difficult as they might appear as horizontal kink oscillations due to projection effects (Wang et al. 2008; Aschwanden 2009).

Horizontal and vertical kink oscillations can be a useful tool for constraining important properties of the localized corona (e.g., magnetic field) using MHD seismology (Nakariakov & Ofman 2001; Arregui et al. 2007; Van Doorselaere et al. 2008). The damping/growth of these waves may also provide clues about the role of dynamic ambient plasma (Ruderman 2011). MHD seismology based on the observations of multiple harmonics of kink waves can lead to estimates of longitudinal density stratification (Andries et al. 2005a, 2005b) and to longitudinal variation and expansion of the magnetic field (see, e.g., Andries et al. 2009 and references therein). Resonant absorption may be one of the potential mechanisms that can explain the observed fast damping of transverse standing and propagating kink waves. The transfer of energy from the transverse motions to the azimuthal Alfvénic motions is essential for the damping by resonant absorption (see, e.g., Hollweg & Yang 1988; Goossens et al. 1992; Ruderman & Roberts 2002; Goossens et al. 2002b, 2006, 2009, 2011, 2012). The transverse kink motions may undergo rapid dissipationless damping because their energy is transferred to the azimuthal Alfvénic motions. The eventual damping of the azimuthal Alfvénic motions is not dissipationless and probably much slower than the dissipationless damping of the transverse motions. This mechanism of dissipationless damping is universal in the sense that it works for both standing and propagating waves (see, e.g., Terradas et al. 2010; Verth et al. 2010; Pascoe et al. 2010, 2012). A concern about resonant absorption as a dissipationless damping mechanism of transverse (horizontal or vertical) kink waves is the lack of the observation of the azimuthal Alfvénic motions in the vicinity of the resonant position. Other potential mechanisms for the damping of the transverse waves may be phase-mixing (Ofman & Davila 1995; Nakariakov et al. 1997), dissipation of kink and Alfvén waves by small-scale turbulence (Nakariakov et al. 1999; Van Ballegoijen et al. 2011), and even the simple relaxation of the active region field lines. Therefore, study of the damping and dissipation of differently polarized transverse kink oscillations in the magnetized solar atmosphere is of significant importance in the context of the coronal heating.

In the present paper, we outline the rare observational evidence of kink vertical transverse oscillation in different parts of a large-scale laminar plasma curtain formed by diffused and unresolved thin loop threads in the off-limb corona of the western equator. This is the first detection of collective vertical transverse oscillations in a large-scale plasma curtain. The large-scale plasma curtain is very different from individual coronal loop strands for which MHD seismology was originally devised. The classic version of MHD seismology almost invariably uses the thin-tube or short wavelength approximation in cylindrical waveguides (Roberts 1981; Aschwanden 2004; compare the review by Andries et al. 2009 and references therein). The detection of vertical oscillations in the present large-scale plasma curtain may require new modeling attempts beyond the existing theoretical approach for tubular waves and MHD seismology (Roberts 1981; Nakariakov & Verwichte 2005). Indeed the spatial dimensions of this large-scale laminar plasma curtain are very long and the inhomogeneity length scales of plasma and magnetic field properties are also far longer than those considered in the presently existing tube-wave theories (Roberts 1981; Nakariakov & Verwichte 2005). The present paper aims

to discuss the detection, possible excitation, and dissipation of the vertical kink oscillations seen in the plasma curtain. The X6.9 flare blast loci on 2011 August 9, situated in the northward direction on the solar disk, generate global disturbances that interact with this magnetized plasma medium asymmetrically and obliquely. These global disturbances most likely excite vertical kink oscillations in the deeper layer as well as at the outer interface of the plasma curtain. The rest of the paper is structured as follows. In Section 2, we describe the observations. In Section 3, we report the detection of vertical kink oscillations and their implications in the observational base line of the Atmospheric Imaging Assembly (AIA) on board *SDO*. In Section 4, we offer a theoretical interpretation of the observed oscillations. The last section is a summary and discussions on the major findings of our paper.

2. OBSERVATIONS

A X6.9-class solar flare was observed in active region AR11263 (N17 W69) at the western equatorial limb on 2011 August 9. The flare started at 07:48 UT with a peak intensity at 08:05 UT. The flare ended at 08:08 UT and is classified as an impulsive event. In the present paper we have used imaging data showing the flare-induced oscillatory dynamics of a laminar plasma curtain formed by unresolved, diffused, and thin loop threads as observed by the AIA on board *SDO*. The large-scale plasma curtain was situated in the off-limb corona near the western equator in the southward direction of the flaring active region (see Figure 1). AIA has a maximum resolution of 0.6 pixel^{-1} and a cadence of 12 s. AIA provides full disk observations of the Sun in three ultra-violet continua at 1600 Å, 1700 Å, 4500 Å, and seven Extreme Ultraviolet (EUV) narrow bands at 171 Å, 193 Å, 211 Å, 94 Å, 304 Å, 335 Å, and 131 Å, respectively (Lemen et al. 2012). Therefore, it provides observations of multi-temperature, high spatial and temporal resolution plasma dynamics in the solar atmosphere. For the current analysis of the flare-induced oscillations of the diffused plasma curtain, we have used the data recorded by AIA 171 Å filter. The image sequence recorded in 171 Å ($\sim T_f = 1.0 \times 10^6 \text{ K}$) reveal information about the inner coronal plasma. The flare-generated global disturbances and these global disturbances in turn triggered the observed vertical transverse oscillations. We use the *SDO*/AIA data to capture the signature of these rare oscillations in the large-scale plasma structure in the solar corona because of the unique position of the magneto-plasma structure almost perpendicular to the line of sight (LOS). To constrain the morphological evolution of large-scale disturbances and creation of the narrow dimming lane above the plasma curtain, we use temporal image data in form of the difference images of 171 Å (cf. Figure 2). The time-series of *SDO*/AIA data has been reduced by the SSW cutout service.³

3. DETECTION OF VERTICAL KINK OSCILLATIONS IN THE LARGE-SCALE LAMINAR PLASMA CURTAIN BY *SDO*/AIA

Figure 1 shows the images of the active region AR 11263 and its surrounding areas on 2011 August 9. *SDO*/AIA 171 Å (left) on 08:07 UT and its difference image (right) show (1) the X6.9 flaring region, (2) the diffused and laminar plasma curtain formed by the unresolved thin loop threads, (3) a narrow off-limb

³ http://lmsal.com/get_aia_data/

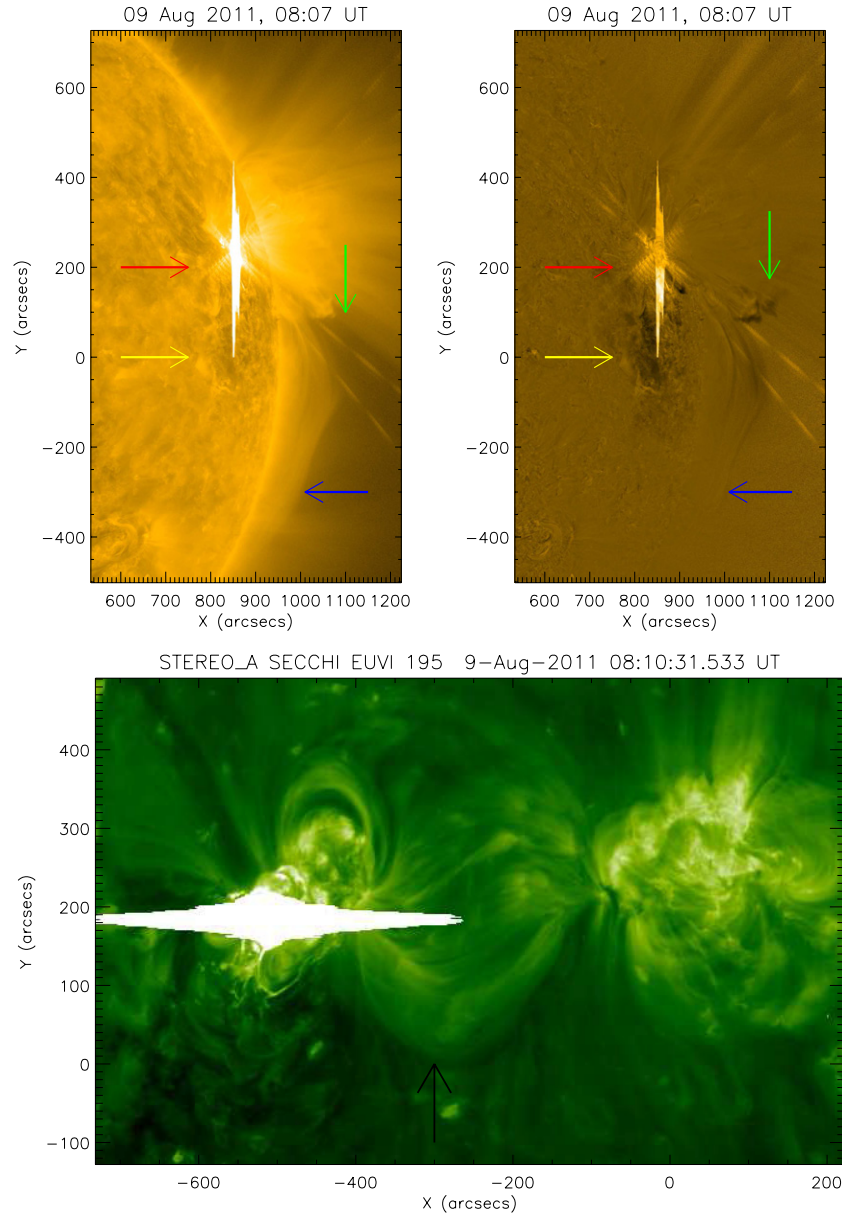


Figure 1. *SDO/AIA* 171 Å (top left) and its difference image (top right), which display the X6.9 flaring region, diffused plasma curtain formed by the unresolved thin loop threads, a narrow off-limb lane of the propagation of flare-generated disturbances, and on-disk large-scale global disturbances shown by red, blue, green, and yellow arrows, respectively. The bottom panel shows the *STEREO-A* EUVI 195 Å image showing the flaring region and western side core loops (indicated by the black arrow) connecting two active regions. However, the less dense and southward-stretched diffused plasma curtain is not visible.

(An animation and a color version of this figure are available in the online journal.)

lane of the propagation of flare-generated disturbances above the curtain, and (4) on-disk large-scale global disturbances with red, blue, green, and yellow arrows, respectively. The difference image of AIA 171 Å on 08:07 with the image of the same field of view (FOV) on 07:50 UT clearly shows a dimming in the form of an EUV coronal wave after the maximum onset and energy release of the X6.9 flare. The wavefront propagates as a global disturbance in the on-disk part in the southeast of the flaring region. However, the wave disturbance does not pass through the plasma curtain directly and some part of the disturbance only propagates through the narrow lane above the plasma curtain. For comparison, we display the *STEREO-A* EUVI 195 Å image at 08:10 UT on 2011 August 9 (Figure 1 bottom panel; Wuelser et al. 2004). AR 11263 with its X-class flare energy release lies near the center in the northeast quadrant of the Sun. It is clearly

evident that the core off-limb loops in the western side of the flaring region partly visible in the *SDO/AIA* FOV, are large-scale diffused loops adjoining the two active regions as shown by the black arrow. However, the large-scale diffused plasma curtain that lies more to the lower north is not visible with *STEREO-A*. This may be due to its lower density and emissions in the on-disk view of *STEREO-A* EUVI 195 Å snapshot. In the *SDO/AIA* FOV, the same plasma curtain is visible off the limb and lies almost perpendicular to the meridional plane and to our LOS. This comparison is to show that the plasma curtain is very different from normal loop systems as it is very diffused on the long spatial scale and has a low density contrast compared to the ambient atmosphere that made it invisible on the solar disk.

Figure 2 shows the time sequence of the difference images in AIA 171 Å channel to examine the evolution of the

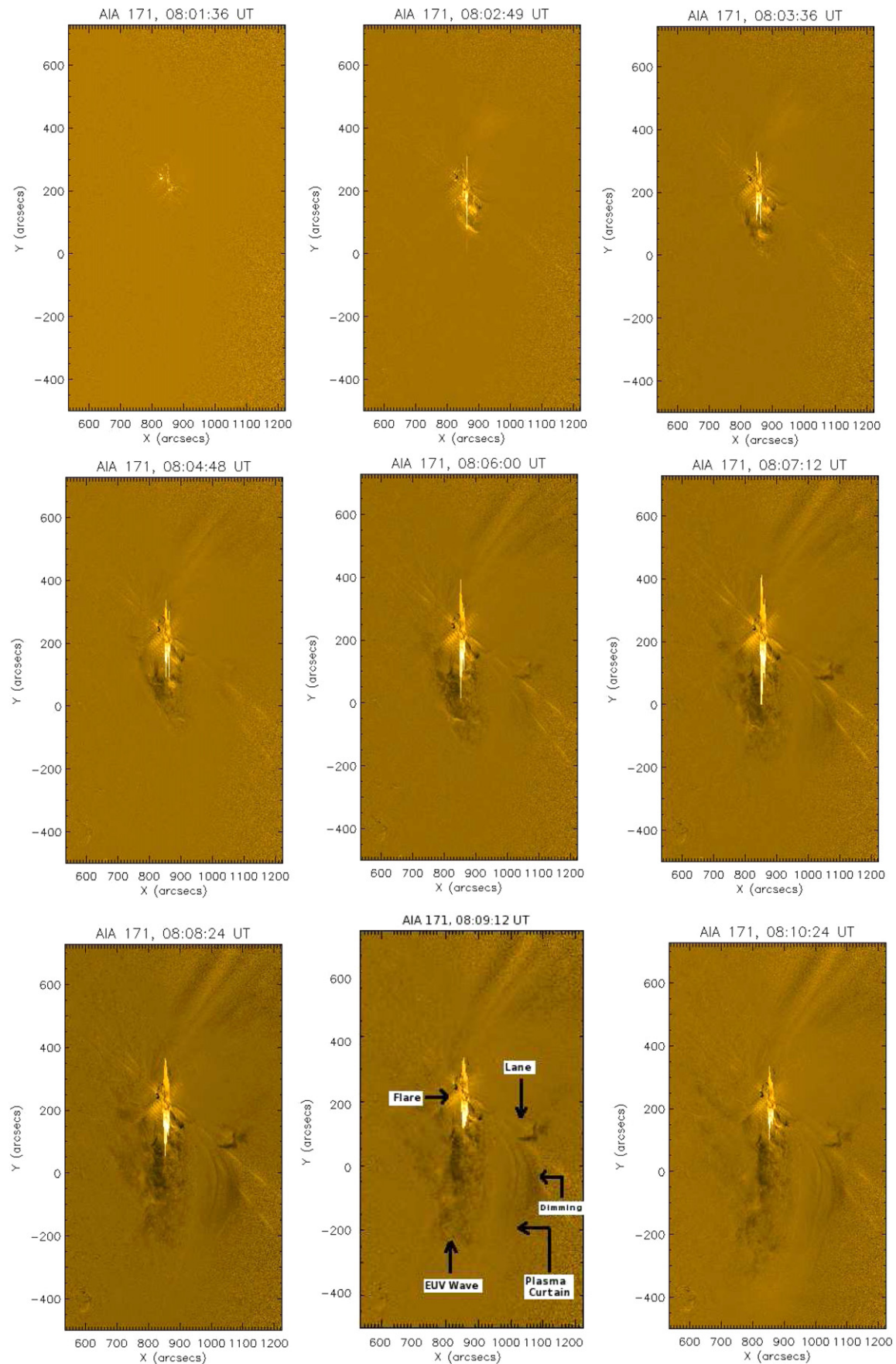


Figure 2. *SDO/AIA* 171 Å difference image sequence showing the generation of the global coronal wave disturbances. Most of the disturbances propagate symmetrically in the southern direction on the disk. However, a narrow lane is also opened above the plasma curtain through which part of the disturbance interacts with it and produces the transverse waves.

(A color version of this figure is available in the online journal.)

large-scale global disturbances and formation of a narrow-dimmed lane at the top of the plasma curtain. After the flare peak energy release at 08:05 UT, the on-disk part of the global EIT wave moves as an almost semi-circular wavefront in the southeast direction with a speed of $\approx 750 \text{ km s}^{-1}$. However, it does not propagate in the form of a symmetric wavefront in the direction of the plasma curtain as observed under the base line of *SDO/AIA* observations. Nevertheless, a narrow dimming region is formed above the plasma curtain that allows the fast moving disturbance to propagate above the surface of the plasma curtain (see snapshot on 08:10 UT). This disturbance pushes the curtain from the upward side to the downward direction, and the vertical transverse oscillations start after 08:10 UT onward in the certain part of the plasma curtain (cf. VTO-*SDO.mpeg*). It should be noted that the triggered oscillations are perpendicular to the LOS almost along the equatorial plane and are thus polarized in the form of vertical transverse oscillations. It should also be noted that the western core loops connecting the two active regions are visible in *STEREO-A* FOV, however, more southwardly stretched plasma curtain and higher parts as visible in *SDO/AIA* of this diffused magnetic structure is unfortunately not visible in *STEREO-A*, most probably due to the less density and emissions. Therefore, we only estimate the oscillatory properties of the fully visible plasma curtain in *SDO/AIA*. Moreover, the unique position of the plasma curtain in the *SDO/AIA* FOV provides us an opportunity to detect these oscillations in the deeper layers as well as at the surface of the plasma curtain. Therefore, to measure and compare the oscillation properties of the deeper layers as well as the surface layers of the plasma curtain, we only use the observations of *SDO/AIA* 171 Å filter data. Let us now investigate the properties of flare-generated vertical transverse oscillations in the large-scale plasma curtain as observed by *SDO/AIA*.

In Figure 3, we display the distance–time diagram (bottom left) along a vertical slit (top left) that is placed vertically over the plasma curtain in the northward side nearer to the flare blast region. The vertical transverse kink oscillations occur in the deeper layer of the curtain, while the surface of the curtain does not show a clear oscillatory signature in a similar way. The distance–time (bottom middle) along a parallel vertical slit (top middle) placed at the middle of the curtain shows vertical oscillations in its deeply rooted layer as well as vertical oscillations of its surface. The distance–time (bottom right) along a parallel vertical slit (top right) placed in the southward region on the opposite side of the curtain near to the flaring region shows oscillations that are only clearly visible at the surface, but that appear to be smoothed out from the deeper layers. We also examined the distance–time map along the path traced out perpendicular to the plasma curtain and parallel to the polar axis (not shown here). We did not find any signature of propagating kink wave trains along the length of the plasma curtain at larger spatial scales at its various heights. This means that only localized vertical kink oscillations are triggered in various parts of the plasma curtain as shown in Figure 3.

In Figures 4 and 5, we display the power spectrum analysis of these oscillations carried out using the standard wavelet technique (Torrence & Compo 1998) and randomization method (Linnell Nemec & Nemec 1985; O’Shea et al. 2001). Let us first look at the vertical oscillations that occur in the deeper layer, which is 30–40 Mm below from the dome-shaped curvilinear outer surface of the plasma curtain. The two panels of Figure 4 show the oscillations at two different spatial parts of the same deeper plasma layer, which is most likely formed by a bunch

of denser and unresolved loop threads (compare the vertical oscillations of the same deeper layer in the bottom left and bottom middle panels of Figure 3). In the first spatial part that lies northward in this layer of the plasma curtain and is closer to the flare blast site, we find vertical oscillations with a period of $\sim 530 \text{ s}$ and a maximum amplitude of about $\pm 4.0 \text{ Mm}$. In the second spatial part that lies southward in this layer of the plasma curtain away from the flare blast site in its middle, we find vertical oscillations with a period of $\sim 795 \text{ s}$ and a maximum amplitude of about 5.0 Mm . Let us now turn to the outer curvilinear surface of the plasma curtain. This acts as magnetic interface between the magnetized and denser plasma curtain and the outer approximately field-free and less dense region. Initially it does not exhibit clear oscillatory motion in its northward part. However, the oscillations are clearly observed near its middle as well as in the southern side of the flare blast region. The observed periods of these oscillations are between 764 and 896 s with maximum amplitudes of $\pm 5.0\text{--}6.0 \text{ Mm}$ (cf. Figure 5). It should be noted that significant oscillatory power is only evident in all these measurements in the intensity wavelet when the transverse oscillations are switched on. The transverse oscillations are not confined to a single thin flux tube, but rather they evolve over several layers of the laminar plasma curtain.

4. INTERPRETATION

We interpret the observed oscillations in the deeper layer of the plasma curtain as vertical kink oscillations. The oscillation with a period of 795 s might be the fundamental kink oscillation. The reason for this suggestion is that in most cases known so far it is the fundamental mode that is excited during a flare energy release. The period of the fundamental mode seems to be rather long compared to the previously detected periods in isolated coronal loops. However, it should be noted that the oscillating part in the middle of the plasma curtain is very long ($L \sim 530 \text{ Mm}$), and the phase speed of the fast mode kink wave (c_k) is $2L/P \sim 1332 \text{ km s}^{-1}$. The plasma curtain has very low density contrast ($\rho_e/\rho_o \sim 1.0$) compared to the background coronal plasma as it is invisible in the on-disk view in the *STEREO* image (cf. Figure 1). Therefore, the observed kink speed c_k of $\sim 1332 \text{ km s}^{-1}$ is almost equal to the internal localized Alfvén speed of the plasma curtain C_{Ao} . This Alfvén speed is comparable to the typical internal coronal Alfvén speed of 1000 km s^{-1} . In the same frame of mind the oscillation with a period of 530 s could be interpreted as the first longitudinal overtone. The period ratio is clearly smaller than 2.0 but that might be caused by stratification of density along the magnetic field (Andries et al. 2005a, 2005b, 2009 and references therein). The fundamental and first overtone are obvious candidates, but we have no hard evidence to claim that the observed oscillations indeed correspond to these modes. If we consider these two vertical kink oscillations as the first two longitudinal harmonics then the ratio of the periods can be used to estimate the density scale height as in Andries et al. (2005a). Here we use the approximation derived by McEwan et al. (2008) for the variation of $P_1/2P_2$ as a function of the ratio of the half loop length ($L/2$) and Λ_c to obtain an estimate for the scale height in the middle part of the plasma curtain where these two oscillations are generated. The length L of this layer along its curved path between two opposite ends is approximately 530 Mm in the projection of the plane. Therefore, the scale height is estimated as $\Lambda_c \sim 88 \text{ Mm}$. The scale height is very close to the typical hydrostatic scale height of the inner corona at 1.0 MK temperature, i.e., $\sim 80 \text{ Mm}$, when we take into account the uncertainty

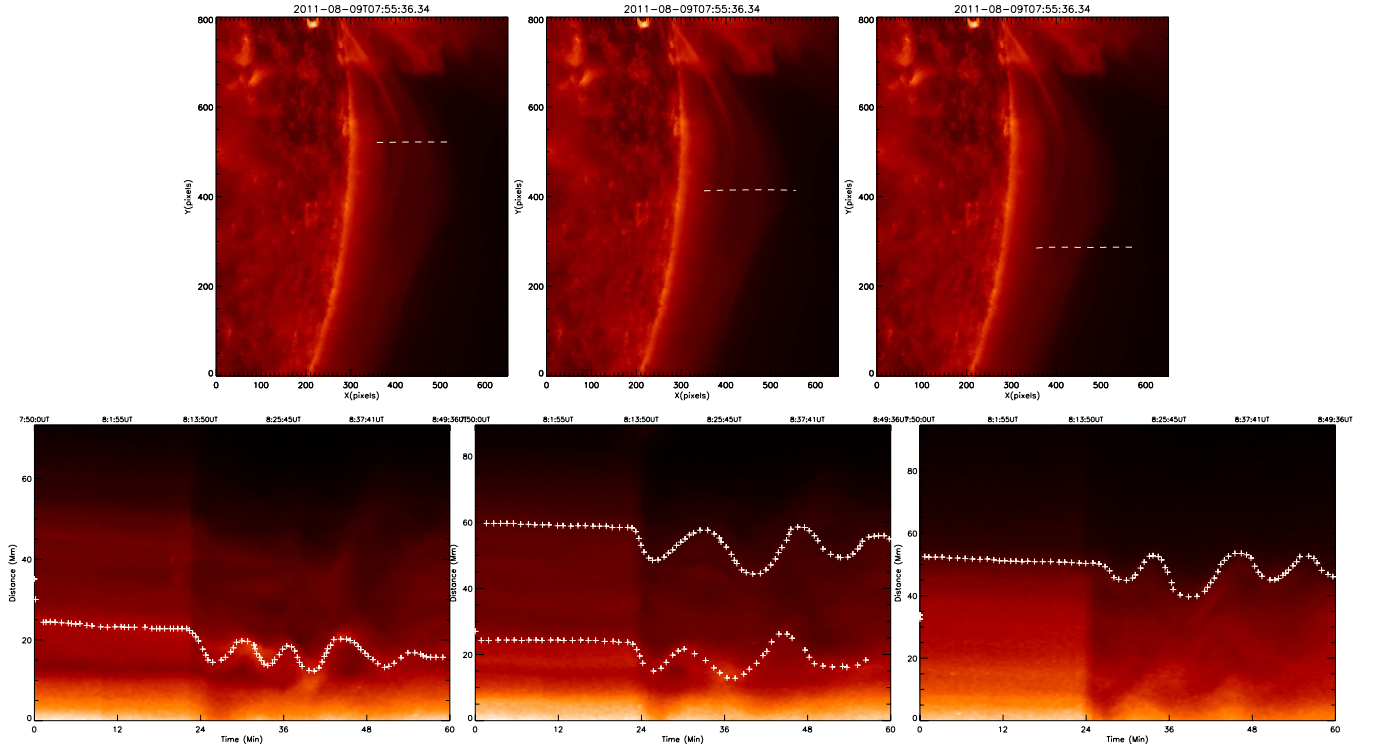


Figure 3. Top three panels show the position of vertical slits over the plasma curtain, while the bottom panels show the corresponding distance–time diagrams. From left to right, the slit positions are shifting away from the flare energy release site.

(A color version of this figure is available in the online journal.)

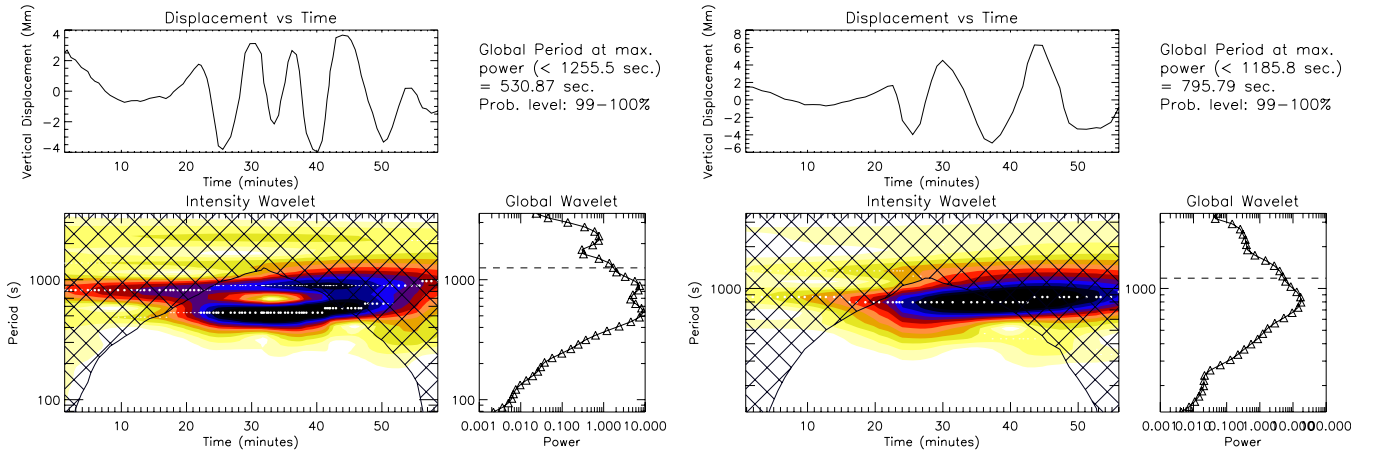


Figure 4. Power spectral analyses of the transverse oscillations of the deep layer of the plasma curtain.

(A color version of this figure is available in the online journal.)

on the estimate of the length of the oscillating part in the middle of plasma curtain. Therefore, we conjecture that this very large plasma curtain is in the hydrostatic equilibrium conditions. This also favors the fact that at the longer spatial scales, the corona can be considered and modeled as a system in the hydrostatic equilibrium. However, deviations from hydrostatic equilibrium are likely to occur in local coronal structures with shorter spatial scales in the form of flux tubes, e.g., isolated loops, coronal X-ray bright points, etc. (e.g., McEwan et al. 2006, 2008; Andries et al. 2009; Srivastava & Dwivedi 2010; Kumar et al. 2011; Luna-Cardozo et al. 2012, and references therein). The amplitudes initially increase in time and subsequently the oscillations suddenly vanish from different spatial positions in the same deeper layer of the plasma curtain. This behavior and

dissipative nature are similar to the well-known fast damping for horizontal transversal standing waves of the coronal loops (Aschwanden et al. 1999; Nakariakov et al. 1999). In the typical solar atmosphere for $\mu = 0.6$ and $\gamma = 1.67$, the magnetic Reynolds number can be approximated as $R_m = 1.9 \times 10^{-8} l_o V_o T_o^{3/2} / \ln \Lambda$ (Priest 1982). For the portion of the observed plasma curtain that, as a whole, undergoes vertical kink oscillations, the length scale, Alfvén velocity, and typical temperature for the formation of Fe IX emission are, respectively, 530 Mm, 1332 km s⁻¹, and 1.0 MK. For the typical inner coronal density of 10^9 cm⁻³ and temperature of 1.0 MK, the column logarithm ($\log \Lambda$) is ~ 19.3 (Priest 1982). Therefore, the magnetic Reynolds number R_m is very high for the observed plasma curtain, which is $\sim 7.0 \times 10^{14}$. This is seven orders of

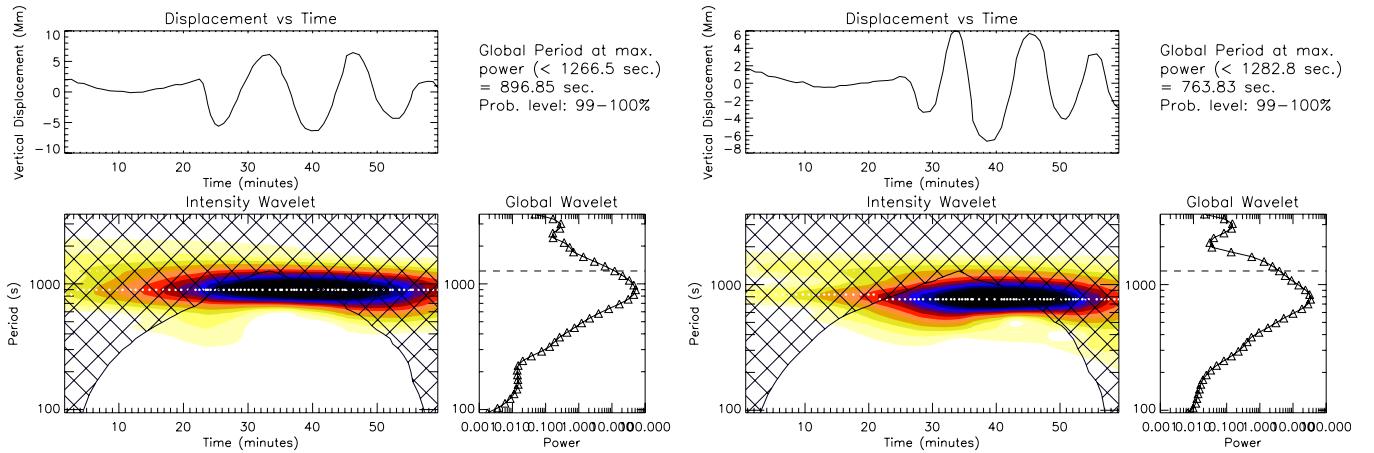


Figure 5. Power spectral analyses of the transverse oscillations of the surface of the plasma curtain at the middle (left) and in its southern direction (right). (A color version of this figure is available in the online journal.)

magnitude higher than the Reynolds number of the environment above a typical photospheric spot, i.e., the coronal loop plasma medium (Priest 1982). This clearly indicates that the collective motion of the plasma is tightly coupled to the magnetic field lines over the length scale of the observed plasma curtain. Therefore, the numerical modeling of the kink oscillations in such plasma curtains needs a very high magnetic Reynolds number environment.

The rapid disappearance of the excited vertical kink oscillations also might be due to a change of angle between the LOS and the plane of the polarization. However, actual damping mechanisms may cause the oscillations to disappear. We will discuss the most plausible candidates for damping and dissipation in the forthcoming sections.

Another possibility is the detection of two independent kink vertical oscillations in two different parts of the same deeper layer of the plasma curtain. The origin of these independent vertical kink oscillations can depend on the energy of the driver, the nature of the interaction with the localized portion of the curtain having specific plasma and magnetic field properties. It is clear that the northward deeper layer, which is near to the flare energy release site, supports comparatively high-frequency (low-period; 530 s) vertical oscillations. This is the location that may serve as the interaction region with a more energetic global wavefront that originated near the flare blast locus. When we examine the same deeper layer situated south of the flare blast locus, we find vertical oscillations with comparatively low frequency (or long periods; 796 s). This is the location that may serve as the interaction region with a comparatively less energetic front of the global disturbance that already lost part of its energy on its way to the solar corona. In the far-south region of the same deeper layer of the curtain, collective vertical oscillations cannot be clearly identified. This region is the remotely positioned interaction region where the global disturbance fails to pump sufficient energy to trigger oscillations. We conjecture that the global disturbance transfers its energy locally to different parts of the plasma curtain depending upon the local plasma and magnetic field conditions there. Hence, the global disturbance excites different vertical oscillatory modes in different regions (Ballai et al. 2005). The study of this interaction is outside of the scope of this paper. These alternative interpretations also seem likely as we could not find any evidence of running kink wave trains across the major axis of the large-scale curtain drawn parallel to

the solar northsouth axis as well as the meridian plane. We only have evidence of localized vertical oscillations in various parts of the curtain as shown in Figure 3.

We do not aim to model the presently observed large-scale system where the oscillations are excited, but we would like to point out what we understand by the term “Laminar Plasma Curtain” system. It cannot be viewed as a single magneto-plasma system since that would violate the equilibrium conditions. On the contrary, as we stated in the beginning, the system is made up of many thin unresolved semi-circular diffused loops and the plasma filling factor is at larger spatial scale than the width of a single average flux tube. The whole structure resembles a large-scale curtain, and the word “laminar” refers to this structuring in the form of unresolved flux tubes. The observed kink motions are the collective antisymmetric transverse motions of the magnetic field and associated plasma. However, these perturbations are distributed over a comparatively longer spatial scale, i.e., in wider regions of the plasma curtain.

Let us focus on the excitation of the vertical transverse waves of the present investigation. The X6.9-class flare in the active region 11263 on 2011 August 9 induces a global large-scale disturbance that propagates in a narrow lane above the plasma curtain and creates a dimming region with lower density. This large-scale propagating disturbance acts as a non-periodic driver that interacts asymmetrically and obliquely with the plasma curtain and triggers waves. This differs from the observations by White et al. (2012). White et al. (2012) observed vertical kink oscillations in a flaring loop with a period of 5.0 minutes. They conjectured that the oscillation is driven by the periodic reconnection and formation of a post-flare hot loop on a scale of a 5.0 minute periodicity and is not due to flare-generated blast waves. Here we observe similar oscillations in a large-scale and diffused plasma curtain triggered by flare-generated global disturbances. Moreover, the observed periods of 795 s and 530 s are quite long compared to the 5.0 minute scale. Although the curtain is formed by laminar arrangements of thin loop threads unfortunately, we cannot resolve them in the present observational base line. The oscillations are triggered unambiguously in that part of the curtain where the plasma layer is slightly denser. This observational situation should also be compared with the numerical findings of Selwa et al. (2011). Selwa et al. (2011) theorized that the amplitude of vertical kink oscillations in a dipolar coronal loop is significantly amplified in comparison to that of horizontal kink oscillations for a

pulse driver that is located symmetrically below the loop. In inclined loops they could not identify vertical kink oscillations. They used this scenario to explain the scarcity of vertical kink oscillations in the corona. Our observations of vertical kink oscillations show a scenario that is completely different from their findings since here the vertical kink oscillations are excited by a non-periodic and non-symmetric driver, i.e., flare-generated global coronal waves.

Let us now turn to the observations of oscillations on the surface of the plasma curtain. There we also observe a vertical kink oscillation with a period between 763 and 896 s. This oscillation is uniformly distributed near the middle and south side of the plasma curtain surface. However, it appears to be absent from the surface of the plasma curtain in the northern side that is nearer to the flare site. The amplitude of this oscillation does not show any signature of decay in the present available observational baseline.

The curtain lies almost in the part of the equator near the west limb, so that the density can be taken to be a smooth function of the radial outward distance inside it. In the deeper layers of the plasma curtain the density is almost constant and the kink waves have predominantly vertical transverse motions. Above the northern surface of the curtain, the dimming is comparatively weak (cf. snapshot 08:10 UT in Figure 2) and the spatial changes in density are smaller inside and outside of the surface. The dimmed region is clearly present near the middle of the surface as well as at the surface in the southward direction. This implies a clear spatial change in density and local Alfvén speed at different spatial locations (north, middle, and south) above the surface of the plasma curtain in the corona assuming that the background magnetic field is constant. This spatial variation of density and local Alfvén speed increases the relative importance of the azimuthal component of the displacement with respect to the radial component at different locations at the surface of the plasma curtain. The vertical kink oscillations that grow at the surface of the plasma curtain during the coronal dimming have velocity components perpendicular to our LOS.

These surface oscillations do not decay while the oscillations in the deeper layers decay in the observational base line of *SDO/AIA*. The reason may be that the continuous dimming due to the passage of fast global disturbances above the curtain creates a low density region. A variation in density in the radial direction can cause damping of standing and propagating waves due to resonant absorption (cf. Goossens et al. 2002b, 2006, 2009, 2011, 2012; Terradas et al. 2010). Density variation along the loop can impede the damping due to resonant absorption or even cause amplification (Soler et al. 2011). Time-dependent variation of the background density counteracts the damping due to resonant absorption of standing waves and can even cause amplification (Ruderman 2011). The cooling and variation of the background plasma properties may also cause damping of the loop kink oscillations (Morton & Erdélyi 2009, 2010a, Morton et al. 2010b, and references therein). However, this scenario is not in support of the present observations as we do not get any signature of cooling of the plasma curtain. Resonant absorption may cause a transfer of energy of the vertical oscillations in the deeper layers toward the outer surface and cause their dissipation. The density decrement above the surface due to dimming may counteract this dissipation by resonant absorption and the oscillations may not be dissipated as observed by *SDO/AIA*. Similar conditions have been observed by Wang et al. (2012) as a coronal dimming above a loop due to CME caused the amplification of kink oscillations. In the present case,

the surface oscillations are not amplified, but remain unchanged and do not undergo dissipation.

5. SUMMARY

Recall that the major concern of this paper is to understand conditions for the excitation of vertical kink waves in a large-scale and diffused plasma curtain. It is clear that the kink waves that are observed in the present study are excited by a large-scale propagating disturbance that acts as a non-periodic driver and interacts asymmetrically and obliquely with the plasma curtain. This mode of excitation differs from that in the observations by White et al. (2012), where the vertical kink waves are excited by a periodic and symmetric driver. There is nothing wrong with vertical kink oscillations excited in two different ways. However, our observations contradict the conjecture by Selwa et al. (2011) that the excitation of vertical kink oscillations requires a driver that is located symmetrically below the loop. Further numerical modeling is needed here keeping the present observations in mind.

The major challenge opened by these first observational findings of vertical kink oscillations in the large-scale plasma curtain, is to try and understand how these waves can be excited in such systems beyond the thin-tube approximation. If different vertical oscillations in different spatial locations of the plasma curtain are generated by one-to-one interactions with global wave energetic fronts, then the evolution of these waves and the transfer of energy depend on the structure of the magnetic field and the composition of the medium in which the waves are generated and propagate. Hence MHD models of kink waves in large-scale plasma structures as observed in our paper need to be developed. The high magnetic Reynolds number plasma environment of the curtain that is almost maintained in hydrostatic equilibrium at larger spatial scales is set in the vertical kink mode oscillations, which are non-decaying at the surface while quickly decaying at deeper layers. The non-decaying and decaying kink oscillations have been recently observed in coronal loops that are driven respectively by the low amplitude continuous and harmonic driver, and high amplitude impulsive driver (Nisticò et al. 2013). Nisticò et al. have reported that impulsive excitation systematically generates transverse perturbations in all loops. We also observe vertical oscillations over larger spatial scales that are generated by the impulsive exciter; however, in our observation, both the decaying and decayless oscillations are associated with the same impulsive driver. Therefore, the opposite nature of the surface oscillations as well as the oscillations in the deeper layer of the plasma curtain indicate the creation of some resonant layers. It is also likely that resonant absorption is at work in decaying the vertical oscillations of the deeper layers of curtain that are associated with the impulsive driver. However, the dimming above its surface most likely counteracts it and keeps the surface oscillations undamped. Detailed theoretical investigations of the excitation and dissipation of such vertical kink oscillations in the large-scale plasma curtain will be the subject of our future work.

In conclusion, we report a very likely physical scenario for unique observations of the vertical transverse waves in a large-scale plasma curtain. However, further studies should be made using spaceborne observations and stringent modeling to shed new light on the physics of these coronal dynamics.

We thank the referee for valuable suggestions that considerably improved the manuscript. We acknowledge the use of

SDO/AIA observations for this study. The data are provided courtesy of NASA/*SDO*, LMSAL, and the AIA, EVE, and HMI science teams. A.K.S. thanks Shobhna Srivastava for her support and encouragement during this work. M.G. acknowledges support from the University of Leuven grant GOA/2009-009 and also partial support from the Interuniversity Attraction Poles Programme initiated by the Belgian Science Policy Office (IAP P7/08 CHARM). A.K.S. acknowledges the support of DST-RFBR (INT/RFBR/P-117) and Indo-Austrian (INT/AUA/BMWF/P-18/2013) project funds during the present research.

REFERENCES

- Andries, J., Arregui, I., & Goossens, M. 2005a, *ApJL*, **624**, L57
- Andries, J., Goossens, M., Hollweg, J. V., Arregui, I., & Van Doorsselaere, T. 2005b, *A&A*, **430**, 1109
- Andries, J., Van Doorsselaere, T., Roberts, B., et al. 2009, *SSRv*, **149**, 3
- Anfinogentov, S., Nakariakov, V. M., Mathioudakis, M., Van Doorsselaere, T., & Kowalski, A. F. 2013, *ApJ*, **773**, 156
- Arregui, I., Andries, J., Van Doorsselaere, T., Goossens, M., & Poedts, S. 2007, *A&A*, **463**, 333
- Aschwanden, M. J. 2004, *Physics of the Solar Corona* (Berlin: Springer-Verlag), 1283
- Aschwanden, M. J. 2009, *SSRv*, **149**, 31
- Aschwanden, M. J., Fletcher, L., Schrijver, C. J., & Alexander, D. 1999, *ApJ*, **520**, 880
- Aschwanden, M. J., & Schrijver, C. J. 2011, *ApJ*, **736**, 102
- Ballai, I., Erdélyi, R., & Pinter, B. 2005, *ApJL*, **633**, L145
- De Moortel, I., & Nakariakov, V. M. 2012, *RSPTA*, **370**, 3193
- Dwivedi, B. N., & Srivastava, A. K. 2006, *SoPh*, **237**, 143
- Erdélyi, R., & Fedun, V. 2007, *Sci*, **318**, 1572
- Erdélyi, R., & Taroyan, Y. 2008, *A&A*, **489**, L49
- Goossens, M. 2008, in *IAU Symp. 247, Waves and Oscillations in the Solar Atmosphere: Heating and Magneto-Seismology*, ed. R. Erdélyi & C. A. Mendoza-Briceno (Cambridge: Cambridge Univ. Press), 228
- Goossens, M., Andries, J., & Arregui, I. 2006, *RSPTA*, **364**, 433
- Goossens, M., Andries, J., & Aschwanden, M. 2002a, *A&A*, **394**, L39
- Goossens, M., Andries, J., Soler, R., et al. 2012, *ApJ*, **753**, 111
- Goossens, M., de Groof, A., & Andries, J. 2002b, in *Proc. IAU Colloq. 188, SP-505 Magnetic Coupling of the Solar Atmosphere*, ed. H. Sawaya-Lacoste (Noordwijk, The Netherlands: ESA), 137
- Goossens, M., Erdélyi, R., & Ruderman, M. 2011, *SSRv*, **158**, 289
- Goossens, M., Hollweg, J. V., & Sakurai, T. 1992, *SoPh*, **138**, 233
- Goossens, M., Terradas, J., Andries, J., Arregui, I., & Ballester, J. L. 2009, *A&A*, **503**, 213
- Gruszecki, M., Murawski, K., Selwa, M., & Ofman, L. 2006, *A&A*, **460**, 887
- Harrison, R. A., Hood, A. W., & Pike, C. D. 2002, *A&A*, **392**, 319
- Hollweg, J. V., & Yang, G. 1988, *JGR*, **93**, 5423
- Jess, D. B., Mathioudakis, M., Erdélyi, R., et al. 2009, *Sci*, **323**, 1582
- Kumar, M., Srivastava, A. K., & Dwivedi, B. N. 2011, *MNRAS*, **415**, 1419
- Lemen, J. R., Title, A. M., Akin, D. J., et al. 2012, *SoPh*, **275**, 17
- Li, Y. P., & Gan, W. Q. 2006, *ApJL*, **644**, L97
- Linnell Nemec, A. F., & Nemec, J. M. 1985, *AJ*, **90**, 2317
- Liu, W., Ofman, L., Nitta, N. V., et al. 2012, *ApJ*, **753**, 52
- Liu, W., Title, A. M., Zhao, J., et al. 2011, *ApJL*, **736**, L13
- Luna-Cardozo, M., Verth, G., & Erdélyi, R. 2012, *ApJ*, **748**, 110
- Mathioudakis, M., Jess, D. B., & Erdélyi, R. 2013, *SSRv*, **175**, 1
- McEwan, M. P., Díaz, A. J., & Roberts, B. 2008, *A&A*, **481**, 819
- McEwan, M. P., Donnelly, G. R., Díaz, A. J., & Roberts, B. 2006, *A&A*, **460**, 893
- McLaughlin, J. A., & Ofman, L. 2008, *ApJ*, **682**, 1338
- Morton, R. J., & Erdélyi, R. 2009, *ApJ*, **707**, 750
- Morton, R. J., & Erdélyi, R. 2010a, *A&A*, **519**, A43
- Morton, R. J., Hood, A. W., & Erdélyi, R. 2010b, *A&A*, **512**, A23
- Morton, R. J., Ruderman, M. S., & Erdélyi, R. 2011, *A&A*, **534**, A27
- Nakariakov, V. M., & Ofman, L. 2001, *A&A*, **372**, L53
- Nakariakov, V. M., Ofman, L., Deluca, E. E., Roberts, B., & Davila, J. M. 1999, *Sci*, **285**, 862
- Nakariakov, V. M., Roberts, B., & Murawski, K. 1997, *SoPh*, **175**, 93
- Nakariakov, V. M., & Verwichte, E. 2005, *LRSP*, **2**, 3
- Nisticò, G., Nakariakov, V. M., & Verwichte, E. 2013, *A&A*, **552**, A57
- Ofman, L., & Davila, J. M. 1995, *JGR*, **100**, 23427
- O'Shea, E., Banerjee, D., Doyle, J. G., Fleck, B., & Murtagh, F. 2001, *A&A*, **368**, 1095
- O'Shea, E., Srivastava, A. K., Doyle, J. G., & Banerjee, D. 2007, *A&A*, **473**, L13
- Pandey, J. C., & Srivastava, A. K. 2009, *ApJL*, **697**, L153
- Pascoe, D. J., Hood, A. W., De Moortel, I., & Wright, A. N. 2012, *A&A*, **539**, A37
- Pascoe, D. J., Wright, A. N., & De Moortel, I. 2010, *ApJ*, **711**, 990
- Priest, E. R. 1982, *Solar Magnetohydrodynamics* (Dordrecht: Reidel), 95
- Roberts, B. 1981, *SoPh*, **69**, 27
- Ruderman, M., & Roberts, B. 2002, *ApJ*, **577**, 475
- Ruderman, M. S. 2011, *SoPh*, **271**, 41
- Selwa, M., Murawski, K., Solanki, S. K., & Wang, T. J. 2007, *A&A*, **462**, 1127
- Selwa, M., & Ofman, L. 2010, *ApJ*, **714**, 170
- Selwa, M., Solanki, S. K., & Ofman, L. 2011, *ApJ*, **728**, 87
- Soler, R., Terradas, J., Verth, G., & Goossens, M. 2011, *ApJ*, **736**, 10
- Srivastava, A. K., & Dwivedi, B. N. 2010, *NewA*, **15**, 8
- Srivastava, A. K., Dwivedi, B. N., & Kumar, M. 2013, *Ap&SS*, **345**, 25
- Terradas, J., Verth, G., & Goossens, M. 2010, *A&A*, **524**, A23
- Torrence, C., & Compo, G. P. 1998, *BAMS*, **79**, 61
- van Ballegoijen, A. A., Asgari-Targhi, M., Cranmer, S. R., & DeLuca, E. E. 2011, *ApJ*, **736**, 3
- Van Doorsselaere, T., Nakariakov, V. M., Young, P. R., & Verwichte, E. 2008, *A&A*, **487**, L17
- Verth, G., Terradas, J., & Goossens, M. 2010, *ApJ*, **718**, 102
- Verwichte, E., Aschwanden, M. J., Van Doorsselaere, T., Foullon, C., & Nakariakov, V. M. 2009, *ApJ*, **698**, 397
- Wang, T., Ofman, L., Davila, J. M., & Su, Y. 2012, *ApJL*, **751**, L27
- Wang, T. J., & Solanki, S. K. 2004, *A&A*, **421**, L33
- Wang, T. J., Solanki, S. K., & Selwa, M. 2008, *A&A*, **489**, 1307
- White, R. S., Verwichte, E., & Foullon, C. 2012, *A&A*, **545**, A129
- Wuelser, J.-P., Lemen, J. R., Tarbell, T. D., et al. 2004, *Proc. SPIE*, **5171**, 111